Direct photon production in d + Au collisions at $\sqrt{s_{NN}} = 200$ GeV

A. Adare,[14] S. S. Adler,[8] S. Afanasiev,[31] C. Aidala,[15,44,45] N. N. Ajitanand,[63] Y. Akiba,[33,57,58] H. Al-Bataineh,[51] A. Al-Jamel,[51] J. Alexander,[63] A. Angerami,[15] K. Aoki,[36,57] N. Apadula,[64] L. Aphecetche,[65] Y. Aramaki,[13,57] R. Armendariz,[51] S. H. Aronson,[8] J. Asai,[57] E. T. Atomssa,[37] R. Averbeck,[64] T. C. Awes,[53] B. Azmoun,[8] V. Babintsev,[25] M. Bai,[7] G. Baksay,[21] L. Baksay,[21] A. Baldisseri,[17] K. N. Barish,[9] P. D. Barnes,[40,*] B. Bassalleck,[50] A. T. Basye,[1] S. Bathe,[6,9,46,58] S. Batsouli,[15,53] V. Baublis,[56] F. Bauer,[9] C. Baumann,[46] A. Bazilevsky,[8,58] S. Belikov,[8,25,29,*] R. Belmont,[69] R. Bennett,[64] A. Berdnikov,[60] Y. Berdnikov,[60] J. H. Bhom,[73] A. A. Bickley,[14] M. T. Bjorndal,[15] D. S. Blau,[35] J. G. Boissevain,[40] J. S. Bok,[73] H. Borel,[17] K. Boyle,[64] M. L. Brooks,[40] D. S. Brown,[51] N. Bruner,[50] D. Bucher,[46] H. Buesching,[8,46] V. Bumazhnov,[25] G. Bunce,[8,58] J. M. Burward-Hoy,[40,39] S. Butsyk,[40,64] C. M. Camacho,[40] X. Camard,[65] S. Campbell,[64] A. Caringi,[47] P. Chand,[5] B. S. Chang,[73] W. C. Chang,[2] J.-L. Charvet,[17] C.-H. Chen,[64] S. Chernichenko,[25] C. Y. Chi,[15] J. Chiba,[33] M. Chiu,[8,15,26] I. J. Choi,[73] J. B. Choi,[11] R. K. Choudhury,[5] P. Christiansen,[42] T. Chujo,[8,68] P. Chung,[63] A. Churyn,[25] O. Chvala,[9] V. Cianciolo,[53] Z. Citron,[64] Y. Cobigo,[17] B. A. Cole,[15] M. P. Comets,[54] Z. Conesa del Valle,[37] M. Connors,[64] P. Constantin,[29,40] M. Csanád,[19] T. Csörgő,[72] J. P. Cussonneau,[65] T. Dahms,[64] S. Dairaku,[36,57] I. Danchev,[69] K. Das,[22] A. Datta,[44] G. David,[8] M. K. Dayananda,[23] F. Deák,[19] H. Delagrange,[65] A. Denisov,[25] D. d'Enterria,[15,37] A. Deshpande,[58,64] E. J. Desmond,[8] A. Devismes,[64] K. V. Dharmawardane,[51] O. Dietzsch,[61] A. Dion,[29,64] M. Donadelli,[61] J. L. Drachenberg,[1] O. Drapier,[37] A. Drees,[64] K. A. Drees,[7] A. K. Dubey,[71] J. M. Durham,[40,64] A. Durum,[25] D. Dutta,[5] V. Dzhordzhadze,[9,66] L. D'Orazio,[43] S. Edwards,[22] Y. V. Efremenko,[53] F. Ellinghaus,[14] T. Engelmore,[15] A. Enokizono,[39,53] H. En'yo,[57,58] B. Espagnon,[54] S. Esumi,[68] K. O. Eyser,[9] B. Fadem,[47] D. E. Fields,[50,58] C. Finck,[65] M. Finger,[10] M. Finger, Jr.,[10] F. Fleuret,[37] S. L. Fokin,[35] B. D. Fox,[58] Z. Fraenkel,[71,*] J. E. Frantz,[15,52,64] A. Franz,[8] A. D. Frawley,[22] K. Fujiwara,[57] Y. Fukao,[36,57,58] S.-Y. Fung,[9] T. Fusayasu,[49] S. Gadrat,[41] I. Garishvili,[66] M. Germain,[65] A. Glenn,[14,39,66] H. Gong,[64] M. Gonin,[37] J. Gosset,[17] Y. Goto,[57,58] R. Granier de Cassagnac,[37] N. Grau,[3,15,29] S. V. Greene,[69] G. Grim,[40] M. Grosse Perdekamp,[26,58] T. Gunji,[13] H.-Å. Gustafsson,[42,*] T. Hachiya,[24] A. Hadj Henni,[65] J. S. Haggerty,[8] K. I. Hahn,[20] H. Hamagaki,[13] J. Hamblen,[66] R. Han,[55] J. Hanks,[15] A. G. Hansen,[40] E. P. Hartouni,[39] K. Haruna,[24] M. Harvey,[8] E. Haslum,[42] K. Hasuko,[57] R. Hayano,[13] X. He,[23] M. Heffner,[39] T. K. Hemmick,[64] T. Hester,[9] J. M. Heuser,[57] P. Hidas,[72] H. Hiejima,[26] J. C. Hill,[29] R. Hobbs,[50] M. Hohlmann,[21] W. Holzmann,[15,63] K. Homma,[24] B. Hong,[34] A. Hoover,[51] T. Horaguchi,[13,24,57,58] D. Hornback,[66] S. Huang,[69] T. Ichihara,[57,58] R. Ichimiya,[57] H. Iinuma,[36,57] Y. Ikeda,[68] V. V. Ikonnikov,[35] K. Imai,[30,36,57] J. Imrek,[18] M. Inaba,[68] M. Inuzuka,[13] D. Isenhower,[1] L. Isenhower,[1] M. Ishihara,[57] T. Isobe,[13,57] M. Issah,[63,69] A. Isupov,[31] D. Ivanischev,[56] Y. Iwanaga,[24] B. V. Jacak,[64,†] J. Jia,[8,15,63,64] X. Jiang,[40] J. Jin,[15] O. Jinnouchi,[57,58] B. M. Johnson,[8] S. C. Johnson,[39] T. Jones,[1] K. S. Joo,[48] D. Jouan,[54] D. S. Jumper,[1] F. Kajihara,[13] S. Kametani,[13,57,70] N. Kamihara,[57,58,67] J. Kamin,[64] M. Kaneta,[58] J. H. Kang,[73] J. Kapustinsky,[40] K. Karatsu,[36,57] M. Kasai,[57,59] K. Katou,[70] T. Kawabata,[13] D. Kawall,[44,58] M. Kawashima,[57,59] A. V. Kazantsev,[35] S. Kelly,[14,15] T. Kempel,[29] B. Khachaturov,[71] A. Khanzadeev,[56] K. M. Kijima,[24] J. Kikuchi,[70] A. Kim,[20] B. I. Kim,[34] D. H. Kim,[48] D. J. Kim,[32,73] E. Kim,[62] E.-J. Kim,[11] E. J. Kim,[62] G.-B. Kim,[37] H. J. Kim,[73] S. H. Kim,[73] Y.-J. Kim,[26] E. Kinney,[14] K. Kiriluk,[14] Á. Kiss,[19] E. Kistenev,[8] A. Kiyomichi,[57] J. Klay,[39] C. Klein-Boesing,[46] D. Kleinjan,[9] H. Kobayashi,[58] L. Kochenda,[56] V. Kochetkov,[25] R. Kohara,[24] B. Komkov,[56] M. Konno,[68] J. Koster,[26] D. Kotchetkov,[9] A. Kozlov,[71] A. Král,[16] A. Kravitz,[15] P. J. Kroon,[8] C. H. Kuberg,[1,*] G. J. Kunde,[40] K. Kurita,[57,59] M. Kurosawa,[57] M. J. Kweon,[34] Y. Kwon,[66,73] G. S. Kyle,[51] R. Lacey,[63] Y. S. Lai,[15] J. G. Lajoie,[29] D. Layton,[26] A. Lebedev,[29,35] Y. Le Bornec,[54] S. Leckey,[64] D. M. Lee,[40] J. Lee,[20] K. B. Lee,[34] K. S. Lee,[34] T. Lee,[62] M. J. Leitch,[40] M. A. L. Leite,[61] B. Lenzi,[61] X. Li,[12] X. H. Li,[9] P. Lichtenwalner,[47] P. Liebing,[58] H. Lim,[62] L. A. Linden Levy,[14] T. Liška,[16] A. Litvinenko,[31] H. Liu,[40,51] M. X. Liu,[40] B. Love,[69] D. Lynch,[8] C. F. Maguire,[69] Y. I. Makdisi,[7,8] A. Malakhov,[31] M. D. Malik,[50] V. I. Manko,[35] E. Mannel,[15] Y. Mao,[55,57] G. Martinez,[65] L. Mašek,[10,28] H. Masui,[68] F. Matathias,[15,64] T. Matsumoto,[13,70] M. C. McCain,[1] M. McCumber,[64] P. L. McGaughey,[40] D. McGlinchey,[14,22] N. Means,[64] B. Meredith,[26] Y. Miake,[68] T. Mibe,[33] A. C. Mignerey,[43] P. Mikeš,[28] K. Miki,[57,68] T. E. Miller,[69] A. Milov,[8,64] S. Mioduszewski,[8] G. C. Mishra,[23] M. Mishra,[4] J. T. Mitchell,[8] A. K. Mohanty,[5] H. J. Moon,[48] Y. Morino,[13] A. Morreale,[9] D. P. Morrison,[8] J. M. Moss,[40] T. V. Moukhanova,[35] D. Mukhopadhyay,[69,71] M. Muniruzzaman,[9] T. Murakami,[36] J. Murata,[57,59] S. Nagamiya,[33] J. L. Nagle,[14,15] M. Naglis,[71] M. I. Nagy,[19,72] I. Nakagawa,[57,58] Y. Nakamiya,[24] K. R. Nakamura,[36,57] T. Nakamura,[24,57] K. Nakano,[57,67] S. Nam,[20] J. Newby,[39,66] M. Nguyen,[64] M. Nihashi,[24] T. Niida,[68] R. Nouicer,[8] A. S. Nyanin,[35] J. Nystrand,[42] C. Oakley,[23] E. O'Brien,[8] S. X. Oda,[13] C. A. Ogilvie,[29] H. Ohnishi,[57] I. D. Ojha,[4,69] M. Oka,[68] K. Okada,[57,58] Y. Onuki,[57] A. Oskarsson,[42] I. Otterlund,[42] M. Ouchida,[24,57] K. Oyama,[13] K. Ozawa,[13] R. Pak,[8] D. Pal,[71] A. P. T. Palounek,[40] V. Pantuev,[27,64] V. Papavassiliou,[51] I. H. Park,[20] J. Park,[62] S. K. Park,[34] W. J. Park,[34] S. F. Pate,[51] H. Pei,[29] V. Penev,[31] J.-C. Peng,[26] H. Pereira,[17] V. Peresedov,[31] D. Yu. Peressounko,[35] R. Petti,[64] A. Pierson,[50] C. Pinkenburg,[8] R. P. Pisani,[8] M. Proissl,[64] M. L. Purschke,[8] A. K. Purwar,[40,64] H. Qu,[23] J. M. Qualls,[1] J. Rak,[29,32,50] A. Rakotozafindrabe,[37] I. Ravinovich,[71] K. F. Read,[53,66] S. Rembeczki,[21] M. Reuter,[64] K. Reygers,[46] V. Riabov,[56] Y. Riabov,[56] E. Richardson,[43] D. Roach,[69] G. Roche,[41] S. D. Rolnick,[9] A. Romana,[37,*] M. Rosati,[29] C. A. Rosen,[14] S. S. E. Rosendahl,[42] P. Rosnet,[41] P. Rukoyatkin,[31] P. Ružička,[28] V. L. Rykov,[57] S. S. Ryu,[73] B. Sahlmueller,[46,64] N. Saito,[33,36,57,58] T. Sakaguchi,[8,13,70] S. Sakai,[68] K. Sakashita,[57,67] V. Samsonov,[56] L. Sanfratello,[50] S. Sano,[13,70] R. Santo,[46] H. D. Sato,[36,57] S. Sato,[8,30,68] T. Sato,[68] S. Sawada,[33] Y. Schutz,[65] K. Sedgwick,[9] J. Seele,[14] R. Seidl,[26,58] A. Yu. Semenov,[29] V. Semenov,[25] R. Seto,[9] D. Sharma,[71] T. K. Shea,[8] I. Shein,[25] T.-A. Shibata,[57,67] K. Shigaki,[24] M. Shimomura,[68] K. Shoji,[36,57] P. Shukla,[5] A. Sickles,[8,64] C. L. Silva,[29,61] D. Silvermyr,[40,53] C. Silvestre,[17] K. S. Sim,[34] B. K. Singh,[4] C. P. Singh,[4] V. Singh,[4]

M. Slunečka,[10] A. Soldatov,[25] R. A. Soltz,[39] W. E. Sondheim,[40] S. P. Sorensen,[66] I. V. Sourikova,[8] F. Staley,[17] P. W. Stankus,[53] E. Stenlund,[42] M. Stepanov,[51] A. Ster,[72] S. P. Stoll,[8] T. Sugitate,[24] C. Suire,[54] A. Sukhanov,[8] J. P. Sullivan,[40] J. Sziklai,[72] S. Takagi,[68] E. M. Takagui,[61] A. Taketani,[57,58] R. Tanabe,[68] K. H. Tanaka,[33] Y. Tanaka,[49] S. Taneja,[64] K. Tanida,[36,57,58,62] M. J. Tannenbaum,[8] S. Tarafdar,[4] A. Taranenko,[63] P. Tarján,[18] H. Themann,[64] D. Thomas,[1] T. L. Thomas,[50] M. Togawa,[36,57,58] A. Toia,[64] J. Tojo,[57] L. Tomášek,[28] Y. Tomita,[68] H. Torii,[24,36,57,58] R. S. Towell,[1] V-N. Tram,[37] I. Tserruya,[71] Y. Tsuchimoto,[24] H. Tydesjö,[42] N. Tyurin,[25] T. J. Uam,[48] C. Vale,[8,29] H. Valle,[69] H. W. van Hecke,[40] E. Vazquez-Zambrano,[15] A. Veicht,[26] J. Velkovska,[8,69] M. Velkovsky,[64] R. Vértesi,[18,72] V. Veszprémi,[18] A. A. Vinogradov,[35] M. Virius,[16] M. A. Volkov,[35] V. Vrba,[28] E. Vznuzdaev,[56] X. R. Wang,[23,51] D. Watanabe,[24] K. Watanabe,[68] Y. Watanabe,[57,58] F. Wei,[29] R. Wei,[63] J. Wessels,[46] S. N. White,[8] N. Willis,[54] D. Winter,[15] F. K. Wohn,[29] C. L. Woody,[8] R. M. Wright,[1] M. Wysocki,[14] W. Xie,[9,58] Y. L. Yamaguchi,[13,57,70] K. Yamaura,[24] R. Yang,[26] A. Yanovich,[25] J. Ying,[23] S. Yokkaichi,[57,58] Z. You,[55] G. R. Young,[53] I. Younus,[38,50] I. E. Yushmanov,[35] W. A. Zajc,[15] O. Zaudtke,[46] C. Zhang,[15,53] S. Zhou,[12] J. Zimányi,[12,*] L. Zolin,[31] and X. Zong[29]

(PHENIX Collaboration)

[1]*Abilene Christian University, Abilene, Texas 79699, USA*

[2]*Institute of Physics, Academia Sinica, Taipei 11529, Taiwan*

[3]*Department of Physics, Augustana College, Sioux Falls, South Dakota 57197, USA*

[4]*Department of Physics, Banaras Hindu University, Varanasi 221005, India*

[5]*Bhabha Atomic Research Centre, Bombay 400 085, India*

[6]*Baruch College, City University of New York, New York, New York 10010, USA*

[7]*Collider-Accelerator Department, Brookhaven National Laboratory, Upton, New York 11973-5000, USA*

[8]*Physics Department, Brookhaven National Laboratory, Upton, New York 11973-5000, USA*

[9]*University of California-Riverside, Riverside, California 92521, USA*

[10]*Charles University, Ovocný trh 5, Praha 1, 116 36 Prague, Czech Republic*

[11]*Chonbuk National University, Jeonju 561-756, Korea*

[12]*Science and Technology on Nuclear Data Laboratory, China Institute of Atomic Energy, Beijing 102413, People's Republic of China*

[13]*Center for Nuclear Study, Graduate School of Science, University of Tokyo, 7-3-1 Hongo, Bunkyo, Tokyo 113-0033, Japan*

[14]*University of Colorado, Boulder, Colorado 80309, USA*

[15]*Columbia University, New York, New York 10027, and Nevis Laboratories, Irvington, New York 10533, USA*

[16]*Czech Technical University, Zikova 4, 166 36 Prague 6, Czech Republic*

[17]*Dapnia, CEA Saclay, F-91191 Gif-sur-Yvette, France*

[18]*Debrecen University, H-4010 Debrecen, Egyetem tér 1, Hungary*

[19]*ELTE, Eötvös Loránd University, H-1117 Budapest, Pázmány P. s. 1/A, Hungary*

[20]*Ewha Womans University, Seoul 120-750, Korea*

[21]*Florida Institute of Technology, Melbourne, Florida 32901, USA*

[22]*Florida State University, Tallahassee, Florida 32306, USA*

[23]*Georgia State University, Atlanta, Georgia 30303, USA*

[24]*Hiroshima University, Kagamiyama, Higashi-Hiroshima 739-8526, Japan*

[25]*IHEP Protvino, State Research Center of Russian Federation, Institute for High Energy Physics, Protvino 142281, Russia*

[26]*University of Illinois at Urbana-Champaign, Urbana, Illinois 61801, USA*

[27]*Institute for Nuclear Research of the Russian Academy of Sciences, prospekt 60-letiya Oktyabrya 7a, Moscow 117312, Russia*

[28]*Institute of Physics, Academy of Sciences of the Czech Republic, Na Slovance 2, 182 21 Prague 8, Czech Republic*

[29]*Iowa State University, Ames, Iowa 50011, USA*

[30]*Advanced Science Research Center, Japan Atomic Energy Agency, 2-4 Shirakata Shirane, Tokai-mura, Naka-gun, Ibaraki-ken 319-1195, Japan*

[31]*Joint Institute for Nuclear Research, 141980 Dubna, Moscow Region, Russia*

[32]*Helsinki Institute of Physics and University of Jyväskylä, P.O. Box 35, FI-40014 Jyväskylä, Finland*

[33]*KEK, High Energy Accelerator Research Organization, Tsukuba, Ibaraki 305-0801, Japan*

[34]*Korea University, Seoul 136-701, Korea*

[35]*Russian Research Center "Kurchatov Institute," Moscow 123098, Russia*

[36]*Kyoto University, Kyoto 606-8502, Japan*

[37]*Laboratoire Leprince-Ringuet, Ecole Polytechnique, CNRS-IN2P3, Route de Saclay, F-91128 Palaiseau, France*

[38]*Physics Department, Lahore University of Management Sciences, Lahore, Pakistan*

[39]*Lawrence Livermore National Laboratory, Livermore, California 94550, USA*

[40]*Los Alamos National Laboratory, Los Alamos, New Mexico 87545, USA*

[41]*LPC, Université Blaise Pascal, CNRS-IN2P3, Clermont-Fd, 63177 Aubiere Cedex, France*

[42]*Department of Physics, Lund University, Box 118, SE-221 00 Lund, Sweden*

[43]*University of Maryland, College Park, Maryland 20742, USA*

[44]*Department of Physics, University of Massachusetts, Amherst, Massachusetts 01003-9337, USA*

[45]*Department of Physics, University of Michigan, Ann Arbor, Michigan 48109-1040, USA*
[46]*Institut fur Kernphysik, University of Muenster, D-48149 Muenster, Germany*
[47]*Muhlenberg College, Allentown, Pennsylvania 18104-5586, USA*
[48]*Myongji University, Yongin, Kyonggido 449-728, Korea*
[49]*Nagasaki Institute of Applied Science, Nagasaki-shi, Nagasaki 851-0193, Japan*
[50]*University of New Mexico, Albuquerque, New Mexico 87131, USA*
[51]*New Mexico State University, Las Cruces, New Mexico 88003, USA*
[52]*Department of Physics and Astronomy, Ohio University, Athens, Ohio 45701, USA*
[53]*Oak Ridge National Laboratory, Oak Ridge, Tennessee 37831, USA*
[54]*IPN-Orsay, Universite Paris Sud, CNRS-IN2P3, B.P. 1, F-91406 Orsay, France*
[55]*Peking University, Beijing 100871, People's Republic of China*
[56]*PNPI, Petersburg Nuclear Physics Institute, Gatchina, Leningrad Region 188300, Russia*
[57]*RIKEN Nishina Center for Accelerator-Based Science, Wako, Saitama 351-0198, Japan*
[58]*RIKEN BNL Research Center, Brookhaven National Laboratory, Upton, New York 11973-5000, USA*
[59]*Physics Department, Rikkyo University, 3-34-1 Nishi-Ikebukuro, Toshima, Tokyo 171-8501, Japan*
[60]*Saint Petersburg State Polytechnic University, St. Petersburg 195251, Russia*
[61]*Universidade de São Paulo, Instituto de Física, Caixa Postal 66318, São Paulo CEP05315-970, Brazil*
[62]*Seoul National University, Seoul, Korea*
[63]*Chemistry Department, Stony Brook University, SUNY, Stony Brook, New York 11794-3400, USA*
[64]*Department of Physics and Astronomy, Stony Brook University, SUNY, Stony Brook, New York 11794-3400, USA*
[65]*SUBATECH (Ecole des Mines de Nantes, CNRS-IN2P3, Université de Nantes), B.P. 20722, 44307 Nantes, France*
[66]*University of Tennessee, Knoxville, Tennessee 37996, USA*
[67]*Department of Physics, Tokyo Institute of Technology, Oh-okayama, Meguro, Tokyo 152-8551, Japan*
[68]*Institute of Physics, University of Tsukuba, Tsukuba, Ibaraki 305, Japan*
[69]*Vanderbilt University, Nashville, Tennessee 37235, USA*
[70]*Waseda University, Advanced Research Institute for Science and Engineering, 17 Kikui-cho, Shinjuku-ku, Tokyo 162-0044, Japan*
[71]*Weizmann Institute, Rehovot 76100, Israel*
[72]*Institute for Particle and Nuclear Physics, Wigner Research Centre for Physics, Hungarian Academy of Sciences (Wigner RCP, RMKI) H-1525 Budapest 114, P.O. Box 49, Budapest, Hungary*
[73]*Yonsei University, IPAP, Seoul 120-749, Korea*

(Received 6 August 2012; revised manuscript received 15 April 2013; published 17 May 2013)

Direct photons have been measured in $\sqrt{s_{NN}} = 200$ GeV $d + \mathrm{Au}$ collisions at midrapidity. A wide p_T range is covered by measurements of nearly real virtual photons ($1 < p_T < 6$ GeV/c) and real photons ($5 < p_T < 16$ GeV/c). The invariant yield of the direct photons in $d + \mathrm{Au}$ collisions over the scaled $p + p$ cross section is consistent with unity. Theoretical calculations assuming standard cold-nuclear-matter effects describe the data well for the entire p_T range. This indicates that the large enhancement of direct photons observed in $\mathrm{Au} + \mathrm{Au}$ collisions for $1.0 < p_T < 2.5$ GeV/c is attributable to a source other than the initial-state nuclear effects.

DOI: 10.1103/PhysRevC.87.054907 PACS number(s): 25.75.Dw

I. INTRODUCTION

Direct photons—emission from processes other than hadronic decays—provide a useful window to investigate the evolution of heavy-ion collisions. Because direct photons are generated throughout all stages of a collision up to chemical freeze-out, the resulting composite momentum spectrum represents the full-time evolution of the hot dense medium. The low-momentum component, typically $1 < p_T < 3$ GeV/c, is of particular interest as a manifestation of thermal photons from the hot partonic phase [1]. The predominant production process for the high p_T direct photon is $q + g \rightarrow g + \gamma$ with a large Q^2 between the incoming partons. The nuclear parton distribution functions (nPDFs) inside a nucleus [2,3] differ from that in a proton. Thus, modification of nPDFs can be probed by high-p_T direct photons.

Direct photons in both $\mathrm{Au} + \mathrm{Au}$ and $p + p$ collisions were measured at the Relativistic Heavy Ion Collider [4–8] over a wide p_T range, which was achieved through measurements of both real photons and nearly real virtual photons [9]. For $1.0 < p_T < 2.5$ GeV/c, a significant excess of direct photons over the binary-scaled $p + p$ yield was observed in central $\mathrm{Au} + \mathrm{Au}$ collisions, suggesting the existence of thermal photons emitted from the hot medium. The key to measurements of the direct photon production for $p_T < 5$ GeV/c is the use of virtual photons, which greatly reduces the background of photons from $\pi^0, \eta \rightarrow 2\gamma$. For $p_T > 4$ GeV/c, real photons are used and previous $\mathrm{Au} + \mathrm{Au}$ measurements [8] indicate agreement with the binary-scaled $p + p$ collisions over $4 < p_T < 22$ GeV/c. However, effects either in the initial state

*Deceased.
†PHENIX spokesperson: jacak@skipper.physics.sunysb.edu

or in the medium created in Au + Au collisions may cancel, making the d + Au measurement crucial to understanding the Au + Au results, because only initial-state effects are present in d + Au collisions.

Cold-nuclear-matter (CNM) effects may play an important role in direct photon production in $A + A$ collisions and possibly modify the production rate compared to $p + p$ collisions. CNM effects in the measured direct photon yield include interplays of various initial-state effects such as the Cronin enhancement [10], isospin effect, modification of nPDFs inside the nucleus, and the initial-state energy loss of colliding partons [11,12]. The d + Au results shed light on these nontrivial effects and are necessary to make a firm statement about thermal photon emission in Au + Au collisions. The CNM effects were studied in d + Au collisions at these energies through measurements of π^0, η, and J/ψ [13–15]; however, direct photons allow studying the initial-state nuclear effects, without the ambiguities of the hadronization process.

In this paper, we present results of direct-photon measurements in $\sqrt{s_{NN}} = 200$ GeV d + Au collisions at midrapidity for $1 < p_T < 16$ GeV/c. Both virtual-photon and real-photon measurements are performed as independent analyses. The virtual-photon analysis uses data taken in 2008 to provide results for the low-p_T region, approximately $1 < p_T < 6$ GeV/c. The real-photon analysis uses data recorded in 2003 for complimentary results above 5 GeV/c. In addition, we report improved direct photon results in $\sqrt{s} = 200$ GeV $p + p$ collisions for $1 < p_T < 5$ GeV/c using 2006 data. The new $p + p$ results are combined with the previously published $p + p$-collision results from 2005 data [4,9] to serve as a reference for the d + Au data.

II. EXPERIMENT AND DATA ANALYSIS

The two central arms of the PHENIX detector [16] cover $|\eta| < 0.35$ in pseudorapidity and $\pi/2$ in azimuthal angle for each arm. Minimum bias (MB) events were triggered by beam-beam counters located at both sides of the interaction point, covering $3.0 < |\eta| < 3.9$, which were also used to determine the event centrality for d + Au collisions. Events containing high-p_T photons and electrons were selectively recorded by photon and single-electron triggers in coincidence with the MB trigger. The photon trigger required an energy deposition in the electromagnetic calorimeter (EMCal) and the electron trigger required a hit in the ring-imaging Čerenkov detector with a correlated, above-threshold, EMCal energy deposition. The virtual-photon analysis used 0.7 nb^{-1} of MB data and 54.9 nb^{-1} of single-electron-triggered data. The analyzed MB and single-photon-triggered data samples for the real-photon analysis were 0.8 and 1.6 nb^{-1}, respectively, where 1 nb^{-1} of d + Au collisions corresponds to 2×197 nb^{-1} of nucleon-nucleon collisions. We also analyzed 4.0 pb^{-1} of the $p + p$ data from the 2006 run to measure the direct photon cross section for $1 < p_T < 5$ GeV/c through the virtual photon analysis.

Electron tracks above 0.2 GeV/c momentum are reconstructed using drift and pad chambers in each of the central arms, with momentum resolution $\sigma_{p_T}/p_T = 1.1\% \oplus 1.16\% \times p_T$. Electrons are identified by requiring hits in the ring-imaging Čerenkov detector and matching the momentum with the energy measured in the EMCal. Electron pairs are used to measure virtual photons using the method described in Refs. [4,9].

A. Virtual-Photon Analysis

Any source of real direct photons also produces nearly real virtual photons, i.e., low-mass e^+e^- pairs, allowing extraction of the real direct photon yield from low-mass e^+e^- pairs. In the virtual photon analysis, e^+e^- pairs with $m_{ee} < 0.3$ GeV/c^2 and pair $p_T > 1$ GeV/c are measured by the two central arms. Electron pairs are formed from combinations of all electrons and positrons with $p_T > 0.3$ GeV/c in an event, and background pairs arising from random combinations, external conversions, correlated background from double Dalitz decays of π^0, η, and jet-induced correlations are removed by analysis techniques as discussed in Ref. [9]. Electron pair mass distributions for different pair p_T ranges, which comprise the virtual direct photon signal and the hadron decay component, are obtained. The inclusive photon yield is determined from the yield of e^+e^- pairs in $m_{ee} \sim 0.05$ GeV/c^2 with the relation of $\frac{d^2n_{ee}}{dm_{ee}} = \frac{2\alpha}{3\pi}\frac{1}{m_{ee}}dn_\gamma$ [9]. The e^+e^- mass distribution for $m_{ee} < 0.3$ GeV/c^2 and $p_T > 1$ GeV/c is decomposed by a two-component fitting procedure described in Ref. [9] using the known shapes of the direct photon and hadron decay components. The direct photon fraction, r_γ = direct γ/inclusive γ, is extracted from the fitting. Multiplying the direct photon fraction by the inclusive photon yield leads to the direct photon yield.

The systematic uncertainties on the direct-photon fraction are estimated from the difference in extracted direct-photon fraction when varying: (1) the particle compositions in the "cocktail" of hadron decay contributions for the fit, (2) the background subtraction of the measured mass distribution, (3) the mass region used for the fit, and (4) the efficiency corrections. The largest uncertainty is attributable to the particle composition of the hadronic cocktail, particularly $\eta/\pi^0 = 0.48 \pm 0.03$ at $p_T > 2$ GeV/c, which is essentially identical to $p + p$ [17]. The resulting uncertainty in the direct-photon fraction owing to η/π^0 is about 20%–30%, and less than 5% are from all other sources. The uncertainty in the e^+e^- pair acceptance correction introduces an additional 9% uncertainty to the inclusive photon yield, which is added in quadrature with the other uncertainties.

Figure 1 shows the measured direct-photon fractions by the virtual-photon analysis in $p + p$, d + Au, Au + Au [4] collisions from left to right. The $p + p$ result is the combination of [4] and the 2006 data. The curves show the expectations from a next-to-leading-order perturbative-quantum-chromodynamics (NLO pQCD) calculation [18,19]. The cutoff mass scale dependence of the calculation is also shown for three cases: $\mu = 0.5p_T$, $1.0p_T$, and $2.0p_T$. With respect to the expectations for d + Au and Au + Au, the same NLO pQCD calculation results are simply scaled by the nuclear-overlap function without considering modification of nPDFs. The nuclear-overlap function is calculated from a Glauber model [20], which is expressed as $T_{dA,AA} = N_{\rm coll}/\sigma_{pp}^{\rm inel}$. Here, $N_{\rm coll}$

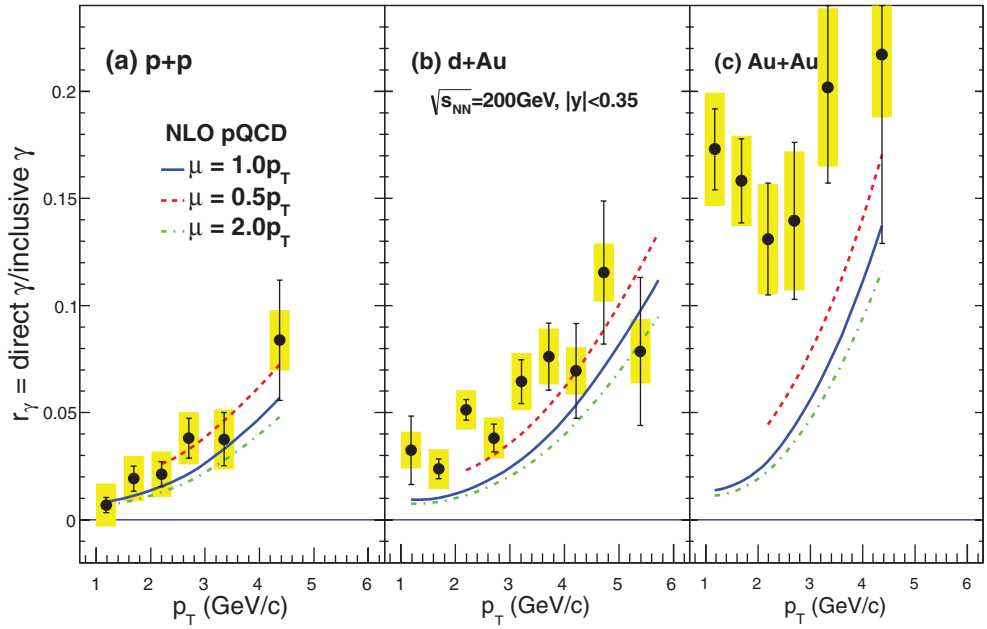

FIG. 1. (Color online) The direct-photon fractions from the virtual-photon analysis as a function of p_T in (a) $p + p$, (b) $d + \mathrm{Au}$, and (c) $\mathrm{Au} + \mathrm{Au}$ (MB) [4] collisions. The statistical and systematic uncertainties are shown by the bars and bands, respectively. The curves show expectations from a NLO pQCD calculation [18,19] with different cutoff mass scales: (solid line) $\mu = 0.5p_T$, (dashed line) $\mu = 1.0p_T$, and (dash-dotted line) $\mu = 2.0p_T$.

is the number of binary nucleon-nucleon collisions and $\sigma_{pp}^{\mathrm{inel}}$ is the cross section of inelastic $p + p$ collisions of 42 mb. The $p + p$ data points were much improved statistically compared to the previously published data, especially above 3 GeV/c, and the $p + p$ result is in good agreement with the NLO pQCD expectations. The $d + \mathrm{Au}$ data are higher than the expectation in $p_T < 4$ GeV/c. Their p_T dependence is similar to the NLO pQCD expectation, unlike the $\mathrm{Au} + \mathrm{Au}$ data.

B. Real-Photon Analysis

While the virtual-photon analysis suffers from low statistics at $p_T > 5.0$ GeV/c, the real-photon analysis is robust at high p_T. The primary detector for the real-photon analysis is the EMCal, which comprises six sectors of lead-scintillator calorimeter and two sectors of lead-glass calorimeter. Contamination from charged hadrons is eliminated by a track-matching veto in the drift chamber, as well as a profile cut on the EMCal shower. Analysis details have been described in Refs. [6,21]. The key to the method is the precise subtraction of the large photonic background originating from hadronic decays, about 80% of which come from $\pi^0 \to 2\gamma$ and about 15% from $\eta \to 2\gamma$. Two techniques, π^0 tagging and statistical subtraction methods, are used to remove decay photons.

The π^0-tagging method identifies neutral pions by reconstructing pairs of photons in the lead-scintillator EMCal sectors that deposit more than 150 MeV. All pairs of photons at least 10 towers ($\approx$0.1 rad) inside the edge of the EMCal which reconstruct to invariant mass $105 < m_{\gamma\gamma} < 165$ MeV are tagged as π^0 decays. The number of direct photons, γ_{dir}, is determined as

$$\gamma_{\mathrm{dir}} = \gamma_{\mathrm{incl}} - (1 + R_{h/\pi^0})(1 + \delta_{\mathrm{miss}})\gamma_{\pi^0 \to 2\gamma}, \qquad (1)$$

where $\gamma_{\mathrm{incl}}, \gamma_{\pi^0 \to 2\gamma}$ are the number of inclusive and π^0 decay photons, respectively, and R_{h/π^0} is the ratio of other hadronic contributions to π^0 decay photons. δ_{miss} represents the probability that either of the photons from $\pi^0 \to 2\gamma$ misses the detector. A fast Monte Carlo (MC) simulation, which includes the geometric acceptance and EMCal response, is used to estimate δ_{miss}. The input p_T distribution of π^0 is taken from $p + p$ collisions [22]. δ_{miss} is then determined as a function of p_T and its uncertainty is evaluated as $\sim$6%–8% by varying the implemented simulation conditions. R_{h/π^0} is calculated using the yield ratios of η and ω to π^0 measured by PHENIX [22,23].

The statistical subtraction method [5,24] is applied to MB-triggered data from both the lead-scintillator and lead-glass EMCal. The hadron decay contribution is estimated by a hadronic cocktail simulation based on the observed p_T spectrum of π^0; other particle spectra are based on the π^0 using m_T scaling [9]. The acceptance and shower merging effects are also implemented in the simulation. A double ratio, R_γ, is calculated as

$$R_\gamma = \left(\frac{dN_\gamma/dp_T}{dN_{\pi^0 \to 2\gamma}/dp_T}\right)^{\mathrm{data}} \Big/ \left(\frac{dN_\gamma/dp_T}{dN_{\pi^0 \to 2\gamma}/dp_T}\right)^{\mathrm{sim}} \qquad (2)$$

An excess owing to direct photons gives $R_\gamma > 1$, and the direct photon yield is determined by $\gamma_{\mathrm{dir}} = (1 - R_\gamma^{-1})\gamma_{\mathrm{incl}}$.

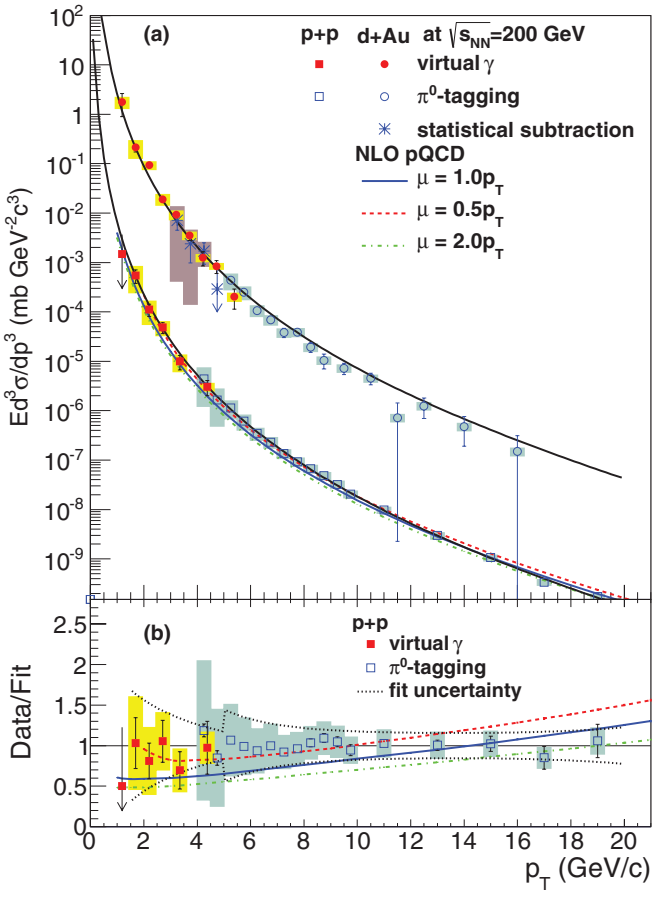

FIG. 2. (Color online) (a) The invariant cross sections of the direct photon in $p+p$ [6,7] and $d+$Au collisions. The $p+p$ fit result with the empirical parameterization described in the text is shown, as well as NLO pQCD calculations, and the scaled $p+p$ fit is compared with the $d+$Au data. The solid and open symbols show the results from the virtual photon and π^0-tagging methods, respectively. The asterisk symbols show the result from the statistical subtraction method for $d+$Au data, overlapping with the virtual photon result in $3 < p_T < 5$ GeV/c. The bars and bands represent the point-to-point and p_T-correlated uncertainties, respectively. (b) The $p+p$ data over the fit. The uncertainties of the fit owing to both point-to-point and p_T-correlated uncertainties of the data are summed quadratically, and the sum is shown as dotted lines. The NLO pQCD calculations divided by the fit are also shown.

III. RESULTS

Figure 2 shows the direct photon cross sections in $p+p$ and $d+$Au collisions from both virtual- and real-photon analyses [7]. The NLO pQCD calculations agree with the $p+p$ data well for a wide p_T range and show a preference for the choice $\mu = 0.5p_T$. Unfortunately, the NLO pQCD calculation with a low-mass cutoff scale less than $1.0p_T$ is not available for $p_T < 2.0$ GeV/c. Thus, we use an empirical parametrization, Eq. (3), inspired by a NLO pQCD formulation for $p+p \to \gamma X$ [19]:

$$E\frac{d^3\sigma}{dp^3} = ap_T^{-(b+c\,\ln x_T)}\left(1-x_T^2\right)^n, \tag{3}$$

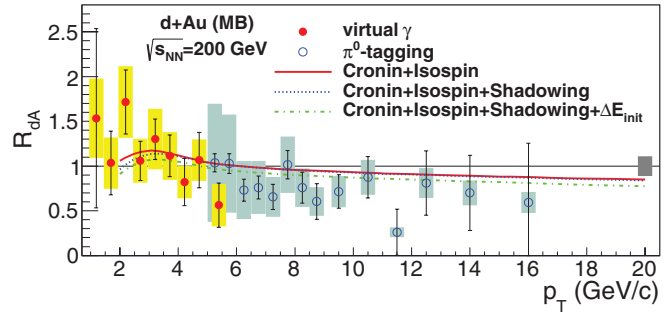

FIG. 3. (Color online) Nuclear modification factor for $d+$Au, R_{dA}, as a function of p_T. The solid and open symbols show the results from the virtual- and real-photon measurements, respectively. The bars and bands represent the point-to-point and p_T-correlated uncertainties, respectively. The box on the right shows the uncertainty of T_{dA} for $d+$Au. The curves indicate the theoretical calculations [26] with different combinations of the CNM effects such as the Cronin enhancement, isospin effect, nuclear shadowing, and initial-state energy loss.

where a, b, c, and n are free parameters and $x_T = 2p_T/\sqrt{s}$. The first factor, $p_T^{-(b+c\,\ln x_T)}$, is a power law with a logarithmic scaling correction, where p_T is given in GeV/c. The convolution of two PDFs in colliding protons consequently introduces the factor, $(1-x_T^2)^n$, which naturally leads to a drop of the cross section to 0 at $x_T = 1$. The virtual-photon ($1.5 < p_T < 5$ GeV/c) and real-photon ($p_T > 5$ GeV/c) results are fit simultaneously, and the point-to-point uncertainty of the data is considered at fitting. The p_T-correlated uncertainty of the fit is identical with that of the data. The quadratic sum of these fit uncertainties is indicated as dotted lines in Fig. 2. The fit describes the data very well for the entire p_T range. The fit parameters with uncertainty (excluding the p_T-correlated uncertainty) are $a = (6.6 \pm 3.3) \times 10^{-3}$ (mb GeV$^{-2}\,c^3$), $b = 6.4 \pm 0.3$, $c = 0.4 \pm 0.2$, and $n = 17.6 \pm 14.9$, with $\chi^2/\mathrm{NDF} = 22.4/16$. The factor of the power law, $b + c\,\ln x_T$, becomes 4.6–5.5 for $0.01 < x_T < 0.1$.

The $d+$Au data illustrate full consistency between the three aforementioned independent analyses. The independent results are in good agreement in the overlap region from $3.0 < p_T < 6.0$ GeV/c. The virtual photon analysis reaches down to 1 GeV/c, and the π^0-tagging method extends to 16 GeV/c. The $d+$Au data are in agreement with the binary collision scaled $p+p$ fit result across the entire p_T coverage. According to the LO pQCD formulation [25], the power of the p_T spectrum in the high-p_T region should be sensitive to the shape of the PDF in the nucleus. A power law fit, Ap_T^{-n}, is performed with the $d+$Au data for $p_T > 8$ GeV/c, as done for $p+p$ ($n = 7.08 \pm 0.09^{\mathrm{stat}} \pm 0.1^{\mathrm{syst}}$) [7] and Au + Au ($n = 7.18 \pm 0.14^{\mathrm{stat}} \pm 0.06^{\mathrm{syst}}$ for most central) [8]. The fit gives a power of $n = 7.17 \pm 0.76^{\mathrm{stat}} \pm 0.01^{\mathrm{syst}}$, consistent with $p+p$ and Au + Au, implying that no significant modification in the shape of the PDFs is observed for $x_T > 0.08$.

Figure 3 shows the nuclear modification factor for $d+$Au, R_{dA}, calculated as the $d+$Au data divided by the

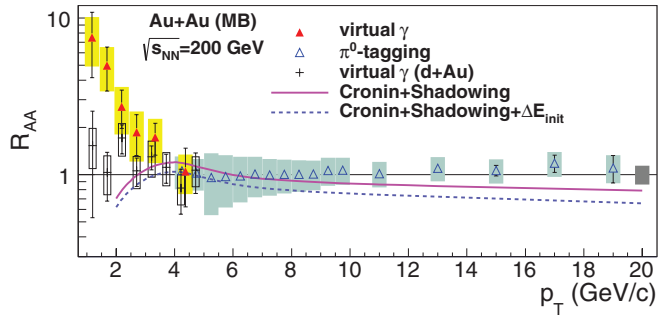

FIG. 4. (Color online) Nuclear modification factors for Au + Au (MB) and $d + \mathrm{Au}$ as a function of p_T. The triangle symbols show results from the (solid) virtual [4] and (open) real photon [8] measurements, respectively. The bars, bands, and boxes represent the same uncertainties as in Fig. 3. The (+) symbols for R_{dA} for $p_T < 5$ GeV/c illustrates the difference in magnitude for R_{AA} between Au + Au and $d + \mathrm{Au}$ collisions. The curves indicate the theoretical calculations [26,28] for Au + Au MB considering only the standard CNM effects.

binary-scaled $p + p$ fit. The point-to-point and p_T-correlated uncertainties of the $p + p$ fit are quadratically summed with those of the $d + \mathrm{Au}$ data points. The sums are shown as bars and bands, respectively. The uncertainty of T_{dA} for $d + \mathrm{Au}$ is indicated by the box located at the right in Fig. 3. R_{dA} is consistent with unity within the reported uncertainty. The theory calculations [26] with different combinations of standard CNM effects are shown with the data. The solid curve is a simple parametrization including only the Cronin enhancement and isospin effect. The nuclear shadowing with the EKS98 parametrization [27] of the nPDFs is additionally considered for the dotted and dash-dotted curves, and the initial state energy loss is included for the dash-dotted curve. For $p_T < 5$ GeV/c, some Cronin enhancement is expected along with minor modifications from nuclear shadowing and initial-state energy loss. At higher p_T, theory predicts a gradual decline in R_{dA} mostly owing to the isospin effect. Within uncertainties, the data are consistent with these theoretical calculations and do not have sufficient precision to resolve the considered initial-state effects across the entire p_T range. The data do, however, rule out much larger effects beyond these standard range predictions. In contrast, Fig. 4 shows that for R_{AA} in Au + Au collisions, there is a much larger enhancement of the direct photon production below 2.0 GeV/c. To clarify the significance of the enhancement in Au + Au compared to $d + \mathrm{Au}$, a constant fit to the $d + \mathrm{Au}$ data for $p_T < 4$ GeV/c is performed. The resulting average R_{dA} in this region is $1.21 \pm 0.12^{\mathrm{stat}} \pm 0.17^{\mathrm{syst}}$. The magnitude of the enhancement in Au + Au reaches as high as $R_{AA} > 7$ at $1.0 < p_T < 1.5$ GeV/c, indicating that there is a significant medium effect on direct photon production in Au + Au.

Furthermore, R_{AA} is consistent with 1 within uncertainties from 4 GeV/c up to 20 GeV/c independent of centrality [8]. While the measured R_{dA} is also consistent with unity, the large uncertainties in the data allow for it to be compatible with the theoretical calculations predicting a gradual decrease owing to the standard CNM effects. The Au + Au predictions from the same theoretical scheme [26,28] considering only the standard CNM effects show a more pronounced suppression at high p_T, which is an effect not apparent in the Au + Au data.

IV. CONCLUSION

In conclusion, direct photons in $1 < p_T < 16$ GeV/c have been measured for $d + \mathrm{Au}$ collisions via three independent analyses, the virtual photon, π^0-tagging, and statistical subtraction methods. The results from these analyses agree in the overlap p_T region. The $p + p$ spectrum has also been improved statistically by the 2006 data. The improved $p + p$ data are parameterized by a pQCD-inspired fit function. The fit describes the data very well for the entire p_T region. R_{dA} is consistent with unity. The data fully support the theoretical calculations with the standard CNM effects for a wide p_T range. R_{AA} shows a much larger enhancement below 2.0 GeV/c compared to the $d + \mathrm{Au}$ data, indicating the existence of a medium effect as an additional source of direct photons.

ACKNOWLEDGMENTS

We thank the staff of the Collider-Accelerator and Physics Departments at Brookhaven National Laboratory and the staff of the other PHENIX participating institutions for their vital contributions. We acknowledge support from the Office of Nuclear Physics in the Office of Science of the Department of Energy, the National Science Foundation, a sponsored research grant from Renaissance Technologies LLC, Abilene Christian University Research Council, Research Foundation of SUNY, and Dean of the College of Arts and Sciences, Vanderbilt University (USA); Ministry of Education, Culture, Sports, Science, and Technology and the Japan Society for the Promotion of Science (Japan); Conselho Nacional de Desenvolvimento Científico e Tecnológico and Fundação de Amparo à Pesquisa do Estado de São Paulo (Brazil); Natural Science Foundation of China (People's Republic of China); Ministry of Education, Youth, and Sports (Czech Republic); Centre National de la Recherche Scientifique, Commissariat à l'Énergie Atomique, and Institut National de Physique Nucléaire et de Physique des Particules (France); Bundesministerium für Bildung und Forschung, Deutscher Akademischer Austausch Dienst, and Alexander von Humboldt Stiftung (Germany); Hungarian National Science Fund, OTKA (Hungary); Department of Atomic Energy and Department of Science and Technology (India); Israel Science Foundation (Israel); National Research Foundation and WCU program of the Ministry Education Science and Technology (Korea); Ministry of Education and Science, Russian Academy of Sciences, and Federal Agency of Atomic Energy (Russia); VR and Wallenberg Foundation (Sweden); the US Civilian Research and Development Foundation for the Independent States of the Former Soviet Union; the US-Hungarian Fulbright Foundation for Educational Exchange; and the US-Israel Binational Science Foundation.

[1] S. Turbide, R. Rapp, and C. Gale, Phys. Rev. C **69**, 014903 (2004).
[2] J. J. Aubert *et al.*, Phys. Lett. B **123**, 275 (1983).
[3] K. J. Eskola, H. Paukkunen, and C. A. Salgado, J. High Energy Phys. 04 (2009) 065.
[4] A. Adare *et al.* (PHENIX Collaboration), Phys. Rev. Lett. **104**, 132301 (2010).
[5] S. S. Adler *et al.* (PHENIX Collaboration), Phys. Rev. Lett. **94**, 232301 (2005).
[6] S. S. Adler *et al.* (PHENIX Collaboration), Phys. Rev. Lett. **98**, 012002 (2007).
[7] S. S. Adler *et al.*, Phys. Rev. D **86**, 072008 (2012).
[8] S. Afanasiev *et al.*, Phys. Rev. Lett. **109**, 152302 (2012).
[9] A. Adare *et al.* (PHENIX Collaboration), Phys. Rev. C **81**, 034911 (2010).
[10] J. W. Cronin *et al.*, Phys. Rev. D **11**, 3105 (1975).
[11] X.-F. Guo and X.-N. Wang, Phys. Rev. Lett. **85**, 3591 (2000).
[12] X.-N. Wang and X.-F. Guo, Nucl. Phys. A **696**, 788 (2001).
[13] S. S. Adler *et al.* (PHENIX Collaboration), Phys. Rev. C **74**, 024904 (2006).
[14] S. S. Adler *et al.* (PHENIX Collaboration), Phys. Rev. Lett. **98**, 172302 (2007).
[15] A. Adare *et al.* (PHENIX Collaboration), Phys. Rev. C **86**, 064901 (2012).
[16] K. Adcox *et al.* (PHENIX Collaboration), Nucl. Instrum. Methods A **499**, 469 (2003).
[17] S. S. Adler *et al.* (PHENIX Collaboration), Phys. Rev. Lett. **96**, 202301 (2006).
[18] L. E. Gordon and W. Vogelsang, Phys. Rev. D **48**, 3136 (1993).
[19] W. Vogelsang (private communication).
[20] M. L. Miller *et al.*, Annu. Rev. Nucl. Part. Sci. **57**, 205 (2007).
[21] S. S. Adler *et al.*, Phys. Rev. C **76**, 034904 (2007).
[22] S. S. Adler *et al.* (PHENIX Collaboration), Phys. Rev. Lett. **91**, 241803 (2003).
[23] A. Adare *et al.* (PHENIX Collaboration), Phys. Rev. C **84**, 044902 (2011).
[24] S. S. Adler *et al.* (PHENIX Collaboration), Phys. Rev. D **71**, 071102 (2005).
[25] H. Fritzsch and P. Minkowski, Phys. Lett. B **69**, 316 (1977).
[26] I. Vitev and B. W. Zhang, Phys. Lett. B **669**, 337 (2008).
[27] K. J. Eskola, V. J. Kolhinen, and C. A. Salgado, Eur. Phys. J. C **9**, 61 (1999).
[28] I. Vitev (private communication).